Resonance Raman detection of carotenoid antioxidants in living human tissue

Igor V. Ermakov
M. Sharifzadeh
Maia Ermakova
W. Gellermann
University of Utah
Department of Physics
Salt Lake City, Utah 84112
E-mail: werner@physics.utah.edu

Abstract. Increasing evidence points to the beneficial effects of carotenoid antioxidants in the human body. Several studies, for example, support the protective role of lutein and zeaxanthin in the prevention of age-related eye diseases. If present in high concentrations in the macular region of the retina, lutein and zeaxanthin provide pigmentation in this most light sensitive retinal spot, and as a result of light filtering and/or antioxidant action, delay the onset of macular degeneration with increasing age. Other carotenoids, such as lycopene and beta-carotene, play an important role as well in the protection of skin from UV and short-wavelength visible radiation. Lutein and lycopene may also have protective function for cardiovascular health, and lycopene may play a role in the prevention of prostate cancer. Motivated by the growing importance of carotenoids in health and disease, and recognizing the lack of any accepted noninvasive technology for the detection of carotenoids in living human tissue, we explore resonance Raman spectroscopy as a novel approach for noninvasive, laser optical carotenoid detection. We review the main results achieved recently with the Raman detection approach. Initially we applied the method to the detection of macular carotenoid pigments, and more recently to the detection of carotenoids in human skin and mucosal tissues. Using skin carotenoid Raman instruments, we measure the carotenoid response from the stratum corneum layer of the palm of the hand for a population of 1375 subjects and develope a portable skin Raman scanner for field studies. These experiments reveal that carotenoids are a good indicator of antioxidant status. They show that people with high oxidative stress, like smokers, and subjects with high sunlight exposure, in general, have reduced skin carotenoid levels, independent of their dietary carotenoid consumption. We find the Raman technique to be precise, specific, sensitive, and well suitable for clinical as well as field studies. The noninvasive laser technique may become a useful method for the correlation between tissue carotenoid levels and risk for malignancies or other degenerative diseases associated with oxidative stress. © *2005 Society of Photo-Optical Instrumentation Engineers.* [DOI: 10.1117/1.2139974]

Keywords: Raman spectroscopy; carotenoids; human skin; macula; antioxidants; noninvasive detection; lutein; zeaxanthin; lycopene; β-carotene.

Paper SS04154RR received Aug. 2, 2004; revised manuscript received Jul. 18, 2005; accepted for publication Jul. 19, 2005; published online Dec. 27, 2005.

1 Introduction

Raman spectroscopy is a highly specific form of vibrational spectroscopy that has long been routinely used to identify and quantify chemical compounds. Carotenoid molecules are especially suitable for Raman measurements since they can be excited with light overlapping their visible absorption bands. Under this excitation condition, they exhibit a very strong resonance Raman scattering (RRS) response, with an enhancement factor of about five orders of magnitude relative to nonresonant Raman spectroscopy.[1] This enables one to detect the characteristic vibrational energy levels of carotenoids through their corresponding spectral fingerprint signature even in complex biological systems, as in living human tissue. Any off-resonance Raman response from other molecules present in the sampling volume would be strongly suppressed under these conditions and would be buried in background noise. Also, the tissue environment of the carotenoids has only a negligible effect on the vibrational energy, thus making the Raman signature virtually identical for the isolated carotenoid molecule, the molecule in solution, or the molecule in a cell environment.

Address all correspondence to Werner Gellermann, Dept. of Physics, University of Utah, 115 S 1400 E Rm. 201, Salt Lake City, UT. Tel: 801–581–5222. Fax: 801–581–4801. E-mail: werner@physics.utah.edu
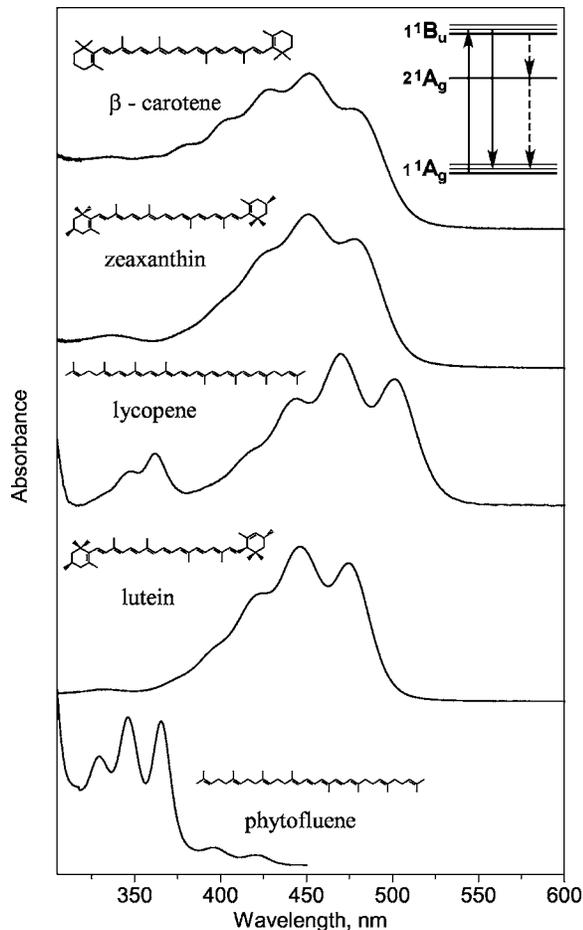
Fig. 1 Absorption spectra, molecular structures, and energy level scheme of major carotenoid species found in human tissue, including β-carotene, zeaxanthin, lycopene, lutein, and phytofluene. Carotenoid molecules, which feature an unusual even parity excited state (see inset). As a consequence, absorption transitions are electric-dipole allowed in these molecules but spontaneous emission is forbidden. The resulting absence of any strong fluorescence in carotenoids is the main reason for the possibility to use RRS, shown as a solid, downward-pointing arrow (optical transition) in the inset, as a noninvasive means of carotenoid detection in human tissue. All carotenoid molecules feature a linear, chainlike conjugated carbon backbone consisting of alternating carbon single (C—C) and double bonds (C=C) with varying numbers of conjugated C=C double bonds, and a varying number of attached methyl side groups. Beta-carotene, lutein, and zeaxanthin feature additional ionone rings as end groups. In beta-carotene and zeaxanthin, the double bonds of these ionone rings add to the effective C=C double bond length of the molecules. Lutein and zeaxanthin have an OH group attached to the ring. Lycopene has 11 conjugated C=C bonds, beta carotene has 11, zeaxanthin has 11, lutein has 10, and phytofluene has 5. The absorptions of all species occur in broad bands in the blue/green spectral range, with the exception of phytofluene, which as a consequence of the shorter C=C conjugation length absorbs in the near UV. Note also, that a small (~10 nm) spectral shift exists between lycopene and lutein absorptions. The spectral shifts can be explored with RRS to selectively detect some of the carotenoids existing as a mixture in human tissues.

Motivated by the growing importance of carotenoid antioxidants in health and disease, and recognizing the lack of any accepted noninvasive technology for the detection of carotenoid antioxidants in living human tissue, we started to
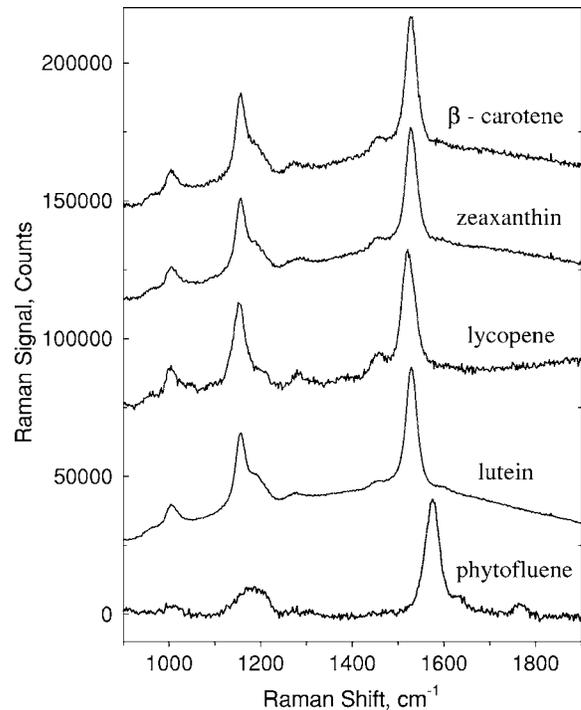

Fig. 2 Resonance Raman spectra of β-carotene, zeaxanthin, lycopene, lutein, and phytofluene solutions, showing the three major "spectral fingerprint" Raman peaks of carotenoids originating from rocking motions of the methyl components (C–CH$_3$) and stretch vibrations of the carbon–carbon single bonds (C—C) and double bonds (C=C). In all carotenoids except phytofluene, these peaks appear at 1008, 1159, and 1525 cm^{-1}, respectively. In phytofluene, the C=C stretch frequency is shifted by ~40 cm^{-1} to higher frequencies. Note the large contrast between Raman response and broad background signal, which is due to the inherently weak fluorescence of carotenoids.

look into RRS as a novel approach for noninvasive, laser-optical detection. Initially, we applied this new method to the detection of macular carotenoid pigments (MPs), which are composed of the carotenoid species lutein and zeaxanthin. Bound to the macular tissue in very high concentrations, these pigments are thought to play a major role in the prevention of age-related macular degeneration.[2] Using RRS in a back-scattering geometry we are developing the technology for in-vivo MP measurements in laboratory and clinical settings.[3–6] Independent trials using the ocular Raman technology for population studies and in connection with ocular pathologies are now in progress at several sites worldwide.[7–12] Recently we have begun to develop RRS spectroscopy for the detection of carotenoid antioxidants in human skin and mucosal tissue,[13–16] tissues where other carotenoid species such as lycopene and beta-carotene are thought to play an important protective role, as in the protection of skin from UV and short-wavelength visible radiation. The carotenoids lutein and lycopene may also have protective functions for cardiovascular health, and lycopene may play a role in the prevention of prostate cancer. It is conceivable that skin levels of these species are correlated with corresponding levels in the internal tissues. Independent clinical studies using Raman detection of skin carotenoids that investigating potential correlations be-
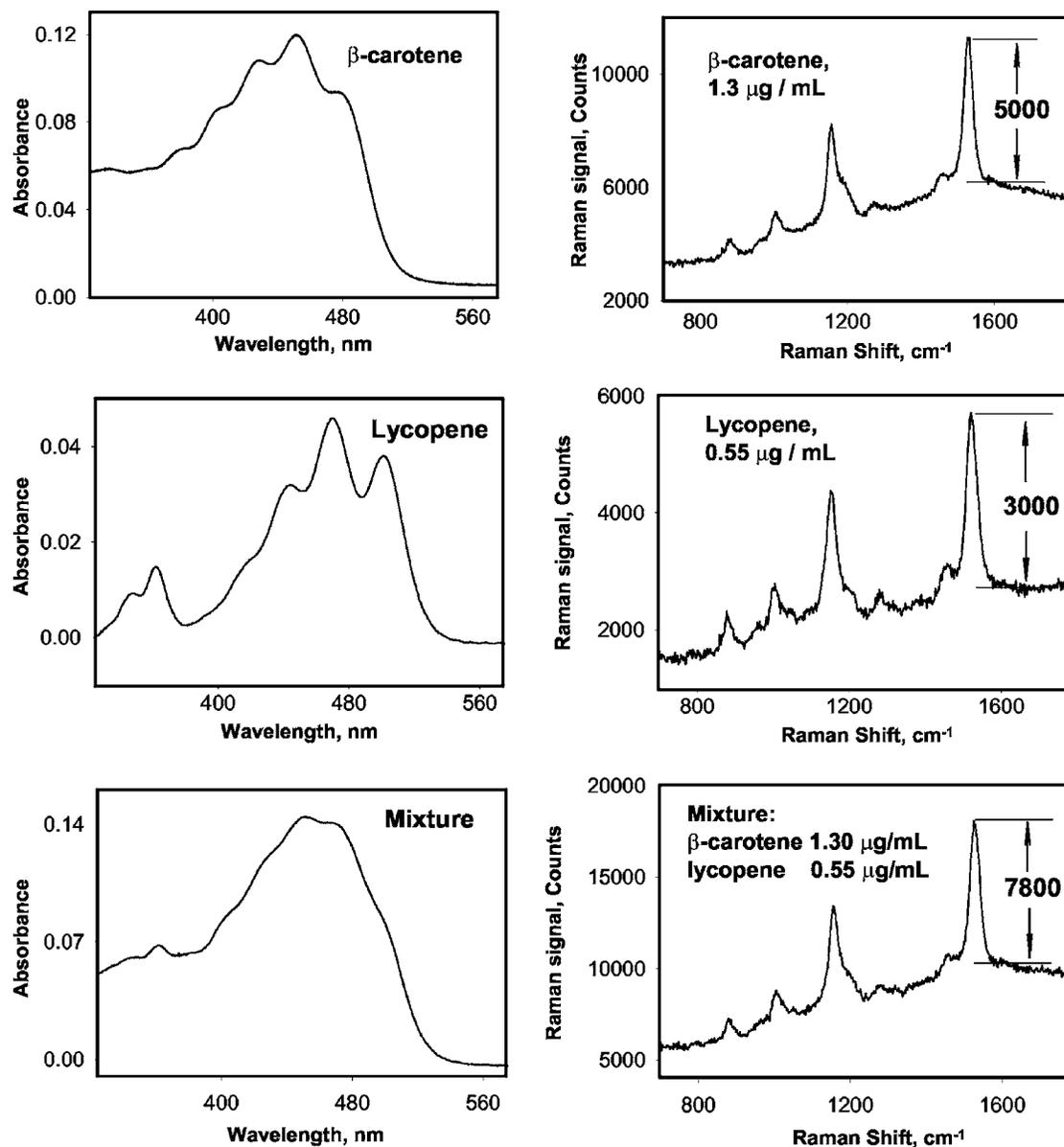
Fig. 3 Absorption spectra and resonance Raman responses for solutions of β-carotenes, lycopenes, and a mixture of both. The Raman response for the mixture corresponds to the sum of responses for individual concentrations, measured with 488 nm excitation. Results demonstrate capability of resonance Raman spectroscopy to detect composite response of several carotenoids if excited at proper spectral wavelength within their absorption bands.

tween skin carotenoid levels and breast and prostate cancer in large subject bases have recently been begun at the Charité Hospital, in Berlin, Germany.[17]

2 Optical Properties and RRS of Carotenoids

Carotenoids are π-electron-conjugated carbon-chain molecules and are similar to polyenes with regard to their structure and optical properties. Distinguishing features are the number of conjugated carbon double bonds ($C=C$ bonds), the number of attached methyl side groups, and the presence and structure of attached end groups. The molecular structures of some of the most important carotenoid species found in human tissue, along with their absorption spectra, are shown in Fig. 1. They include β-carotene, zeaxanthin, lycopene,

lutein, and phytofluene. The electronic absorptions are strong in each case, occur in broad bands ($\sim$100 nm width), and shift to longer wavelength with increasing number of effective conjugation length of the corresponding molecule. The absorption of phytofluene (five conjugated $C=C$ bonds) is positioned in the near UV; β-carotene, lutein, and zeaxanthin (11,10, and 11 $C=C$ bonds, respectively) are centered at $\sim$440 nm, and lycopene (11 bonds) peaks at $\sim$450 nm. All absorptions show a clearly resolved vibronic substructure due to weak electron-phonon coupling, with a spacing of $\sim$1400 cm^{-1}. Strong, electric-dipole allowed absorption transitions occur between the molecules' delocalized π orbitals from the 1 ^1A_g singlet ground state to the 1 ^1B_u singlet excited state (see inset of Fig. 1).

In all cases, optical excitation within the $1\,^1A_g \rightarrow 1\,^1B_u$ absorption band leads to only very weak luminescence transitions[3] (not shown). The extremely low quantum efficiency of the luminescence is caused by the existence of a second excited singlet state, a $2\,^1A_g$ state, which lies below the $1\,^1B_u$ state (see Fig. 1 inset). Following excitation of the $1\,^1B_u$ state, the carotenoid molecule relaxes very rapidly, within[18] ~200 to 250 fs, via nonradiative transitions, to this lower $2\,^1A_g$ state from which electronic emission to the ground state is parity-forbidden (dashed, downward pointing upper arrow in inset of Fig. 1). The resulting low $1\,^1B_u \rightarrow 1\,^1A_g$ luminescence efficiency (10^{-5} to 10^{-4}), and the absence of $2\,^1A_g \rightarrow 1\,^1A_g$ fluorescence of the molecules, enables one to detect the RRS response of the molecular vibrations (shown as solid, downward pointing arrow in inset of Fig. 1) without potentially masking fluorescence signals. Specifically, RRS detects the stretching vibrations of the polyene backbone as well as the methyl side groups.[1]

For tetrahydrofuran solutions of the carotenoids of Fig. 1 we obtain the RRS spectra shown in Fig. 2. Beta-carotene, zeaxanthin, lycopene, and lutein all have strong and clearly resolved Raman signals superimposed on a weak fluorescence background, with three prominent Raman Stokes lines appearing[1] at ~1525 (C=C stretch), 1159 (C=C stretch), and 1008 cm^{-1} (C–CH$_3$ rocking motions). In the shorter chain phytofluene molecule, only the C=C stretch appears, and it is shifted significantly to higher frequencies (by ~40 cm^{-1}).

Raman scattering does not require resonant excitation, in principle, and is therefore suitable to simultaneously detect the vibrational transitions of all Raman active compounds in a given sample. However, off-resonant Raman scattering is a very weak optical effect, requiring intense laser excitation, long signal acquisition times, and highly sensitive, cryogenically cooled detectors. Also, in biological systems, the spectra tend to be very complex due to the diversity of compounds present. This scenario changes drastically if the compounds exhibit absorption bands due to electronic dipole transitions of the molecules, particularly if these are located in the visible wavelength range. When illuminated with monochromatic light overlapping one of these absorption bands, the Raman scattered light will exhibit a substantial resonance enhancement. In the case of carotenoids, 488-nm argon laser light provides an extraordinarily high resonant enhancement of the Raman signals[1] of the order of 10^5. No other biological molecules found in significant concentrations in human tissues exhibit similar resonant enhancement at this excitation wavelength, so *in vivo* carotenoid RRS spectra are remarkably free of confounding Raman responses.

Raman scattering is a linear spectroscopy, meaning that the Raman scattering intensity I_S scales linearly with the intensity of the incident light I_L as long as the scattering compound can be considered as optically thin. Furthermore, at fixed incident light intensity I_L, and as long as the scatterers can be considered as optically thin, the Raman response scales with the population density of the scatterers $N(E_i)$ in a linear fashion according to[3]
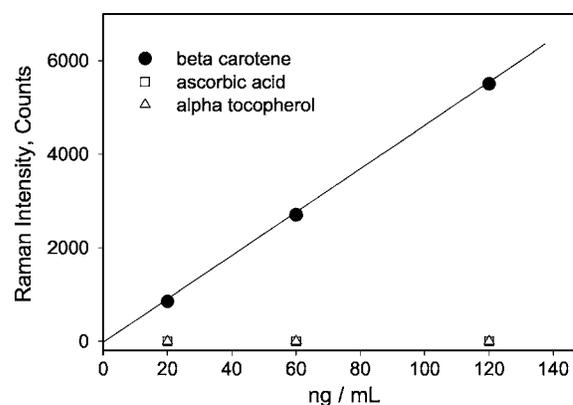

Fig. 4 RRS responses in the spectral vicinity of the C=C stretching frequency, measured for various antioxidants as a function of concentration in ethanol under identical excitation and detection conditions—●, β-carotene; □, ascorbic acid; △, α-tocopherol—from Ref. 13. Note the absence of a Raman response for noncarotenoid compounds.

$$I_s = N(E_i) \times \sigma_R \times I_L.$$

Here, σ_R is a constant whose magnitude depends on the excitation and collection geometry. In optically thick media, as in geometrically thin but optically dense tissue, a deviation from the linear Raman response of I_s versus concentration N can occur, of course—for example, due to self-absorption of the Stokes Raman line by the strong electronic absorption. In general, this can be taken into account, however, at least over a limited concentration range, by calibrating the Raman response with suitable tissue phantoms.

RRS spectroscopy has an additional advantage over ordinary Raman spectroscopy in the possibility to influence the Raman response by judicious choice of the excitation wavelength. This enables one to selectively enhance the Raman response of one carotenoid species over another one in a mixture of compounds. For example, exciting a mixture of phytofluene and lutein at 450 nm would only result in a RRS response from lutein (see Fig. 1), thus enabling us to selectively quantify lutein in this mixture.

Several carotenoid species are usually present in complex biological tissues. For quantification of the composite RRS response it is therefore important to account for individual RRS responses of the excited species. Since the RRS response, in general, follows the absorption line shape, the individual RRS response depends on the extent of the overlap of the excitation laser with the absorption. In the case of equal Raman scattering cross sections, realized when exciting all carotenoids at their respective absorption maxima, the RRS responses should add. To verify this assumption, we measured RRS spectra for solutions of β-carotene, lycopene, and a mixture of both. The results are shown in Fig. 3 for solutions with carotenoid concentrations that are higher than typical physiological concentrations encountered in human tissue, and we see that the RRS response for the carotenoid is roughly equal to the sum of the responses for the individual concentrations.

The specificity of RRS for carotenoid detection is illustrated in Fig. 4, where the RRS response in the C=C stretch frequency range is shown for fresh solutions of β-carotene
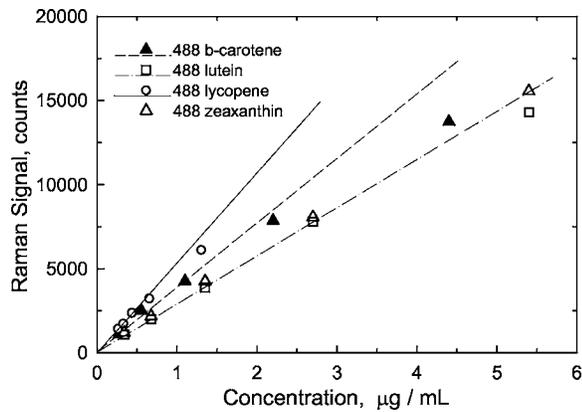
Fig. 5 RRS response of various carotenoid solutions under 488-nm excitation, shown as a function of increasing concentrations—filled triangle, β-carotene; open triangle, zeaxanthin; open square, lutein; and open circle, lycopene. The response is linear up to ~5 μg/mL, which is a carotenoid concentration exceeding that found in human skin. Slight variations in the slopes for each carotenoid solution are in very good agreement with their respective excitation efficiencies. Note the near coincidence of responses for lutein and zeaxanthin.

together with the noncarotenoid compounds ascorbic acid and α-tocopherol. While the Raman response of the carotenoid solution increases with increasing concentration, no Raman response is observed for the noncarotenoid antioxidants.

To assess the relative RRS response for various carotenoids found in human tissue such as skin, we prepared ethanolic solutions of β-carotene, lutein, zeaxanthin, and lycopene, and measured their response over a large concentration range. The results are shown in Fig. 5 and reveal a linear response over a very large concentration range that exceeds the concentrations of carotenoids found in human skin. Slight variations in the slopes for the sampled carotenoid solutions are in very good agreement with their respective excitation efficiencies.

3 Raman Detection of Macular Pigments

3.1 Macular Pigments and Existing Measuring Methods

It has been hypothesized that the macular carotenoid pigments lutein and zeaxanthin[19,20] might play a role in the treatment and prevention of age-related macular degeneration[21,22] (AMD). In the United States, this leading cause of blindness affects ~30% of the elderly over age 70. Analysis of Age-Related Eye Disease Study (AREDS) data reported at recent clinical meetings has confirmed the initial epidemiological findings of the Eye Disease Case Control study[23,24] that high intakes of fruits and vegetables rich in lutein and zeaxanthin are associated with a significantly lower relative risk of AMD. The results were convincing enough that an AREDS II study is planned that will incorporate lutein and/or zeaxanthin supplementation in a large-scale randomized placebo controlled prospective clinical trial. Chemically analysis [high-performance liquid chromatography (HPLC)] of human cadaver eyes with and without a known history of AMD likewise demonstrates a correlation between low levels of
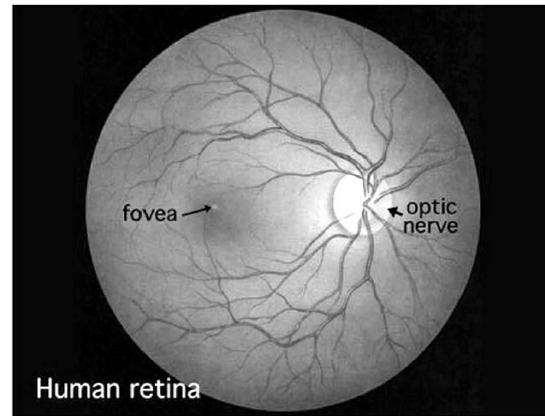
(a)
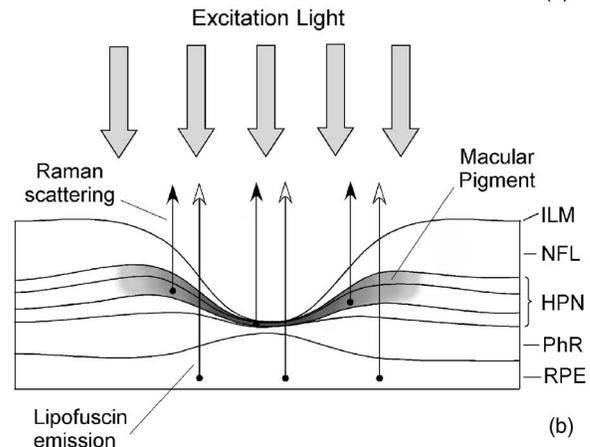
(b)

Fig. 6 (a) Fundus photograph of healthy human retina, showing optic nerve head (bright spot at left) and macula [dark shaded area outlining macular pigment (MP) distributions], and (b) schematic representation of retinal layers participating in light absorption, transmission, and scattering of excitation and emission light: ILM, inner limiting membrane; NFL, nerve fiber layer; HPN, Henle fiber, plexiform, and nuclear layers; PhR, photoreceptor layer; RPE, retinal pigment epithelium. In Raman scattering, the scattering response originates from the MP, which is located anteriorly to the photoreceptor layer. The influence of deeper fundus layers such as the RPE is avoided. In autofluorescence spectroscopy, light emission of deeper fundus layers, such as lipofuscin emission from the RPE, can be stimulated on purpose to generate an instrinsic "light source" for single-path absorption measurements of anteriorly located MP layers (see text).

lutein and zeaxanthin and risk[25] of AMD, and recent flicker photometry and resonance Raman clinical studies reached the same conclusion.[6,26]

Spectroscopic studies of tissue sections of primate maculae [the central 5 to 6 mm of the retina, see Fig. 6(a)] indicate that there are very high concentrations of carotenoid pigments, shown as shaded area in Fig. 6(b), in the Henle fiber layer of the fovea and smaller amounts in the inner plexiform layer,[27] [see Fig. 6(b)]. The mechanisms by which these two macular pigments, derived exclusively from dietary sources such as green leafy vegetables and orange and yellow fruits and vegetables, might protect against AMD is still unclear. They are known to be excellent free-radical-scavenging antioxidants in a tissue at high risk of oxidative damage due to the high levels of light exposure, and abundant highly unsaturated
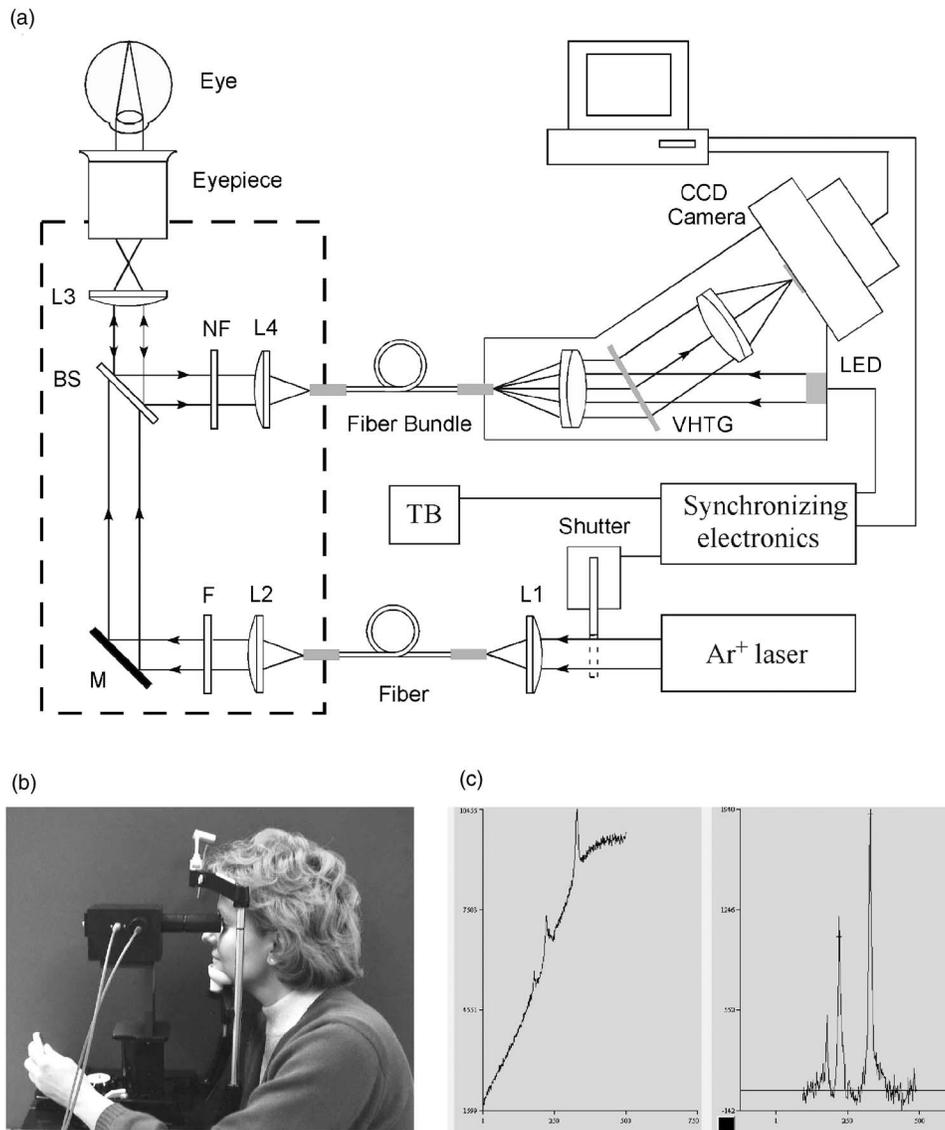
Fig. 7 (a) Schematic diagram of macular pigment resonance Raman detector designed for human clinical studies. Light from an argon laser is routed via optical fiber into an optical probe head (outlined by dashed line) and from there into the eye of a subject where it is projected as ~1 mm diameter spot onto the retina. L1 to L4, lenses; F, laser line filter; BS: dichroic beamsplitter; NF, notch filter; VHF, volume holographic grating; and LED, red-light-emitting diode for visualization of fiber bundle. Raman scattered light is collected in backscattering geometry with lens L3, split off by BS, and sent into a spectrograph via fiber bundle for light dispersion. A CCD array is used to detect the spectrally dispersed light. The instrument is interfaced to a personal computer for light exposure control, data acquisition, and processing. Typical settings are 1 mW of 488-nm laser light for 0.2 s with a 1-mm spot size on the macula. (b) Subject looking into the optical probe head of the instrument. (c) Typical Raman spectra from the retina of a healthy volunteer, measured with dilated pupil (8 mm), and displayed on the computer monitor of the instrument. Left panel, spectrum obtained after a single measurement, clearly showing the carotenoid Raman signals superimposed upon a broad fluorescent background; right panel, same enlarged spectrum obtained after fitting background with a fourth-order polynomial and subtracting it from original spectrum. For quantitation of MP concentration the software displays the Raman response of the strongest peak, corresponding to the C=C stretch, as an intensity score.

lipids.[21,22,28,29] In addition, since these molecules absorb in the blue-green spectral range, they act as filters that may attenuate photochemical damage and/or image degradation caused by short-wavelength visible light reaching the retina.[30]

There is considerable interest to measure MP levels noninvasively in the elderly population to determine[26] whether or not low levels of MP are associated with increased risk of AMD. Currently, the most commonly used noninvasive method for measuring human MP levels is a subjective psy-chophysical heterochromatic flicker photometry test involving color intensity matching of a light beam aimed at the fovea and another aimed at the perifoveal area.[31] However, this method is rather time consuming and requires an alert, cooperative subject with good visual acuity, and it may exhibit a high intrasubject variability when macular pigment densities are low or if significant macular pathology is present.[32] Thus, the usefulness of this method for assessing macular pigment levels in the elderly population most at risk for AMD is se-
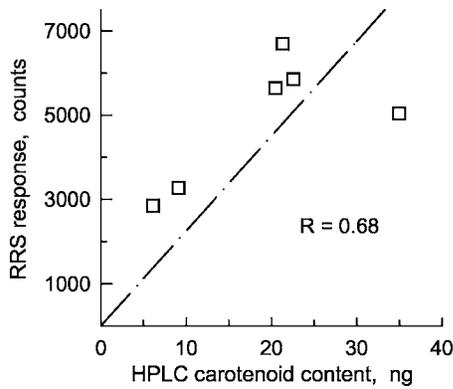
Fig. 8 Correlation of RRS signals obtained for the C=C double bond vibration at 1525 cm^{-1} with the carotenoid content of six monkey retinae as determined by HPLC. A linear fit to the data results in a correlation coefficient of 0.68.
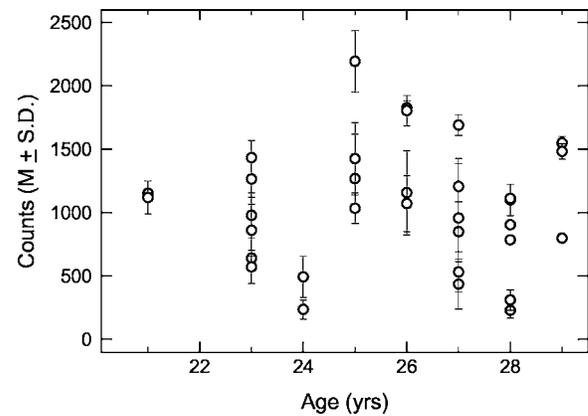

Fig. 9 RRS MP measurements of 33 normal eyes for a young group of subjects ranging in age from 21 to 29 years. Note the large (~10-fold) variation of RRS levels between individuals. Since the ocular transmission properties in this age group can be assumed to very similar, the variations are can be assigned to differing MP levels. Subjects with extremely low carotenoid levels may be at higher risk of developing macular degeneration later in life.

verely limited. Nevertheless, researchers have used flicker photometry to investigate important questions such as variation of macular pigment density with age and diet. In a recent flicker photometry study, for example, the pigment density was found to increase slightly with age,[33] while other studies found the opposite trend.[34]

A number of objective techniques for the measurement of MP in the human retina have been explored recently as alternatives to the subjective psychophysical tests. The underlying optics principles of these techniques are either based on fundus reflection or fundus fluorescence (autofluorescence) spectroscopy. In traditional fundus reflectometry, which uses a light source with a broad spectral continuum, reflectance spectra of the bleached retina are separately measured for fovea and perifovea. The double-path absorption of MP is extracted from the ratio of the two spectra by reproducing its spectral shape in a multiparameter fitting procedure using appropriate absorption and scattering profiles of the various fundus tissue layers traversed by the source light.[35–38] One of the imaging variants of fundus reflectometry uses a TV-based imaging fundus reflectometer with sequential, narrow-bandwidth light excitation over the visible wavelength range and digitized fundus images.[39] Another powerful variant uses a scanning laser ophthalmoscope,[40,41] employing raster-scanning of the fundus with discrete laser excitation wavelengths to produce highly detailed information about the spatial distribution[42–46] of MP (and photopigments). In autofluorescence spectroscopy, lipofuscin in the retinal pigment epithelium is excited with light within and outside the wavelength range of macular pigment absorption. Measuring the lipofuscin fluorescence levels for fovea and perifovea, an estimate of the single-pass absorption of MP can be obtained.[47,48] In a recent study, comparing reflectometry, scanning laser opthalmoscopy (SLO) and flicker photometry in the measurement of macular lutein uptake, SLO was found to be superior to spectral fundus reflectance while psychophysical measurements yielded widely varying results.[38,49]

3.2 Ocular Raman Measurements

We have investigated RRS as a novel approach[2] for the measurement of MP levels in living eyes.[50,51] The technique is

objective as well as noninvasive, appears to be fast and quantitative, and its specificity for carotenoids means that it could be used for patients with a variety of ocular pathologies.

In vivo RRS spectroscopy in the eye takes advantage of several favorable anatomical properties of the tissue structures encountered in the light scattering pathways. First, the major site of macular carotenoid deposition in the Henle fiber layer is of the order of only 100 μm of thickness.[27] This provides a chromophore distribution very closely resembling an optically thin film having no significant self-absorption of the illuminated or scattered light. Second, the ocular media (cornea, lens, vitreous) are generally of sufficient clarity not to attenuate the signal, and they should require appropriate correction factors only in cases of substantial pathology such as visually significant cataracts. Third, since the macular carotenoids are situated anteriorly in the optical pathway through the retina [see Fig. 6(b)], the illuminating light and the backscattered light never encounter any highly absorptive pigments such as photoreceptor rhodopsin and RPE melanin, while the light unabsorbed by the macular carotenoids and the forward- and side-scattered light will be efficiently absorbed by these pigments.[3] In contrast, emission of lipofuscin used in autofluorescence (AF)-based measurements of MP must traverse the photoreceptor layer [see Fig. 6(b)].

Our initial "proof-of-principle" studies of ocular carotenoid resonance Raman spectroscopy employed a laboratory-grade high-resolution Raman spectrometer and flat-mounted human cadaver retinas, human eyecups, and a few whole frog eyes. We were able to record characteristic carotenoid RRS spectra from these tissues with a spatial resolution of approximately 100 μm, and we were able to confirm linearity of response by extracting and analyzing tissue carotenoids by HPLC after completion of the Raman measurements.[2] For *in vivo* experiments and clinical use, we developed a new instrument with lower spectral resolution but highly improved light throughput. The latest instrument version, shown schematically in Fig. 7(a), consists of a low-power air-cooled argon laser, which projects a 1-mm-diam, 1.0-mW, 488-nm spot
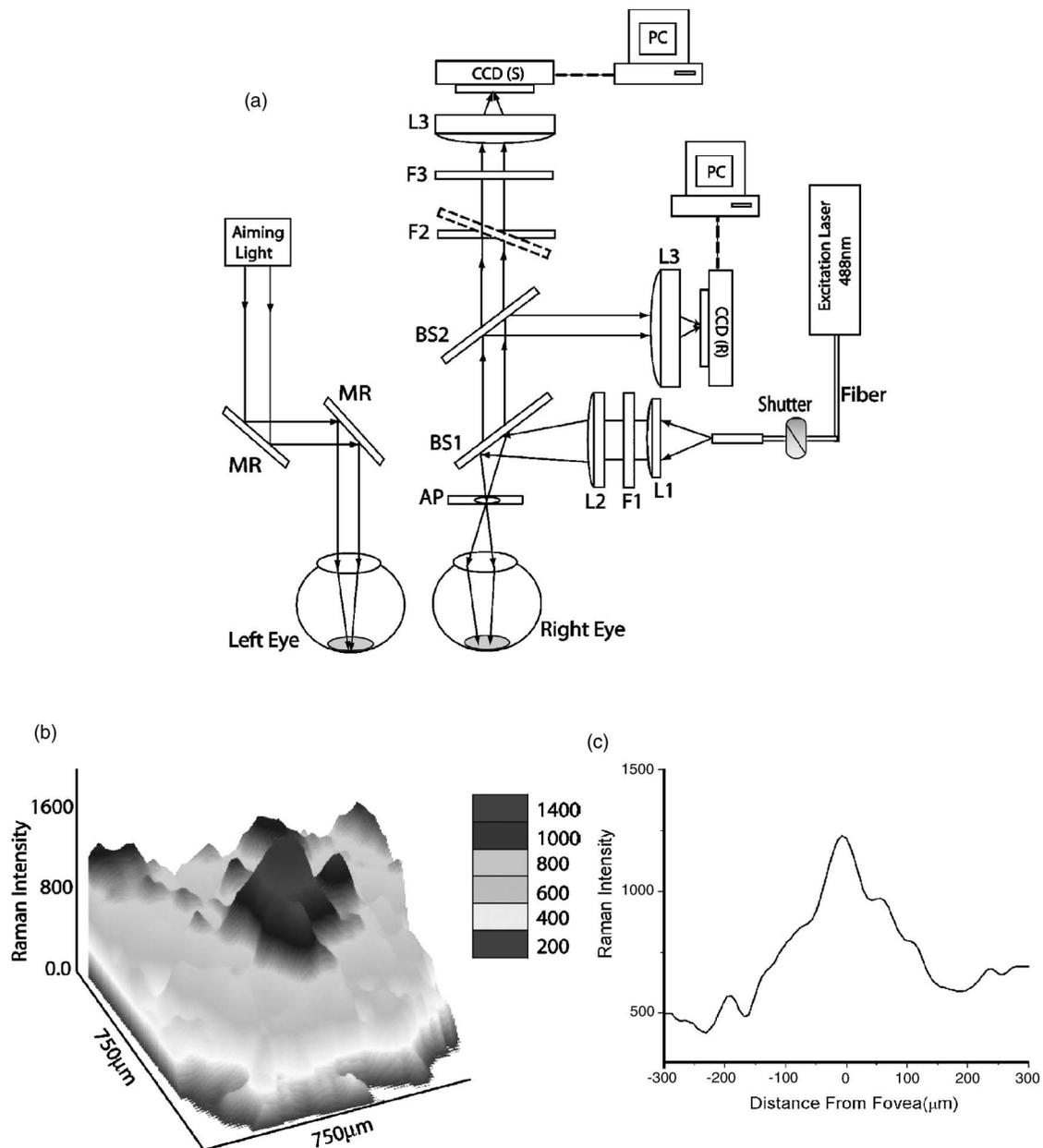
Fig. 10 (a) Schematic diagram used for resonance Raman imaging of the MP distribution of volunteer subjects. Light from blue and green excitation laser wavelengths is sequentially projected onto the retina of a subject as a ~5-mm-diam spot, while the fellow eye is looking at a fixation target. The Raman-scattered light is collimated by the eye lens and imaged simultaneously onto the 2-D arrays of two separate digital imaging CCD cameras, using a beamsplitter (QBS) to generate two separate light paths. One of the cameras images the spatial distribution of the excitation light (reference), while the other camera images light levels in the spectral range of the C=C stretch Raman peak. A rotatable, narrowband filter (F2) is used to selectively realize C=C on-peak and off-peak transmission for the scattered light. Following the registration of an on-peak and an off-peak image, the two images are digitally subtracted (following alignment using vessel landmarks) and displayed as topographic pseudocolor images or surface plots showing the spatial distribution of MP concentrations. L1 to L3: lenses; F1, laser line filter; BS, dichroic beam splitters; F2, tunable filter; F3, bandpass filter. (b) Pseudocolor surface plot of MP distribution in a living human eye measured with out Raman imaging instrument. Raman intensities are coded according to the intensity scale shown on the upper right-hand side of the image. Note the roughly circularly symmetric MP distribution in the central area of the fovea but the appearance of side bumps in peripheral areas. (c) Line scan of the image, in (b) obtained by plotting intensities along a horizontal meridional line running through the center of the macular pigment distribution. The width at half maximum is about 150 μm in this individual.

onto the foveal region for 0.2 s through a pharmacologically dilated pupil.[4] Light backscattered at 180 deg is collimated with a lens, the light scattered at the laser excitation wavelength is rejected by a high efficiency bandpass filter, and the remainder is routed via fiber optics to a Raman spectrograph/ CCD camera combination. The instrument is interfaced to a personal computer equipped with custom-designed software that can subtract background fluorescence and quantify the intensity of the Raman peaks. Living human subjects were asked to fixate on a suitable target to ensure self-alignment,
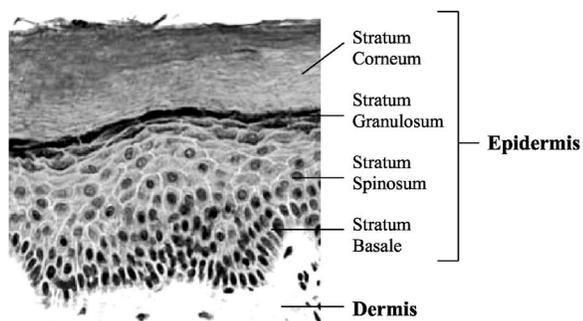
Fig. 11 Layer structure of human skin as seen in a microscope after staining, showing the morphology of dermis, basal layer, stratum spinosum, stratum granulosum, and stratum corneum. Cells of the stratum corneum have no nucleus (missing dark stain spots) and form a relatively homogeneous optical medium well suited for Raman measurements.

while in monkey experiments, we used an additional video monitoring system and red laser aiming beam to confirm foveal targeting. The instrument could be calibrated against solutions of lutein and zeaxanthin in optically thin 1-mm quartz cuvettes placed at the focal point of a lens whose power duplicated the refractive optics of the human eye. Detector response was linear up until optical densities of nearly 0.8, well past carotenoid levels normally encountered in the human macula. Using living monkey eyes, linearity of response at "eye safe" laser illumination levels could again be established relative to HPLC analysis, as we can see from Fig. 8, where we plotted the RRS response of six monkey retinae versus HPLC derived data.[3]

Typical RRS spectra, measured from the macula of a healthy human volunteer, measured with dilated pupil, are shown in Fig. 7(c). The left panel of this figure shows a typical spectrum obtained from a single measurement and clearly reveals carotenoid Raman signals superimposed on a weak and spectrally broad fluorescence background. The background is caused partially by weak intrinsic fluorescence of carotenoids, and partially by the short-wavelength emission tail of lipofuscin fluorophors deposited in the retinal pigment epithelial layer. The ratio between the intensities of the carotenoid C=C Raman peak and the fluorescence background is high enough ($\sim$0.25) that it is easily possible to quantify the amplitude of the C=C peak after digital background subtraction [right panel of Fig. 7(c)]. Carotenoid RRS spectra collected from the living human macula were indistinguishable from the spectra originating from RRS spectra solutions of pure lutein or zeaxanthin solutions.[6]

3.3   Laser Safety Considerations

To comply with ANSI safety regulations, the ocular exposure levels used in our Raman instrument have to stay below certain specified threshold levels. According to the latest issue,[52] ANSI Z136.1-2000, ocular exposure levels must be limited to protect the eye both from photochemically and thermally induced retinal injury under the measurement conditions (visible light near 0.5 μm, immobilized eyes, exposure time of 0.25 s). The photochemical limit for retinal injury (Sec. 8.3.1 of ANSI guidelines) is listed as 2.7 C_B J/cm^2, where C_B is a

wavelength correction factor, and results in 15.5 J/cm^2, using C_B=5.75 for 488 nm. The thermal limit for retinal injury (Sec. 8.3.2.), valid for an exposure time $0.07 < t < 0.7$ s, must be calculated from the laser spot present at the cornea, and is listed as $1.8(\alpha/1.5)t^{0.75}$ mJ/cm^2. Here, α is the angle of the laser source at the location of the viewer, measured in milliradians. Using t=0.07 s and α=58.8$\times$10^{-3} rad, we obtain an energy density of 9.6 mJ/cm^2 at the cornea for the thermal exposure limit of the retina.

In a typical single-exposure measurement with our instrument (0.25-s ocular exposure with 1-mW light at 488 nm), a total laser energy of 0.25 mJ is projected onto an 8-mm-diam spot at the cornea, and a 1-mm-diam spot on the retina. This corresponds to a retinal exposure level of 32 mJ/cm^2, which is 480 times lower than the 15.5-J/cm^2 photochemical limit. For the used ocular exposure, we calculate a level of 0.5 mJ/cm^2, considering that the light energy of 0.25 mJ is distributed over a spot size diameter of 8 mm at the cornea; therefore, this exposure level is 19 times below the thermal limit of 9.6 mJ/cm^2 for retinal injury.

3.4   Clinical Results

We measured the macular carotenoid pigment levels of hundreds of human subjects at the Moran Eye Center of the University of Utah using RRS spectroscopy. Most patients can readily perform the test with acceptable intrasession and intersession repeatability of ±10% as long as they have preserved central fixation (typically a visual acuity of 20/80 or better). The subjects noted a central afterimage from the laser illumination after each measurement that they felt was similar to that of a camera flash. This afterimage usually faded within a minute or two. Subjects with dense media opacities such as visually significant cataracts or with poor pupillary dilation of $<$6 mm were usually excluded from measurements in our clinical studies because we found their measurements to be artifactually low.

When we measured a large population of normal subjects, none of whom were consuming supplements containing substantial amounts of lutein or zeaxanthin, we found a striking decline of average macular carotenoid levels with age,[3] a phenomenon sometimes observed with other MP measurement techniques.[12,53] Part of this decline can be explained by "yellowing" of the crystalline lens with age, which would attenuate some of the illuminating and backscattered light, but we also found consistently low MP levels even in patients who had previously had cataract surgery with implantation of optically clear prosthetic intraocular lenses[3] (pseudophakia). Also, we noted that patients with unilateral cataracts after trauma or retinal detachment repair typically have very similar RRS carotenoid levels in the normal and in the pseudophakic eye. Thus, we concluded that there is a decline of macular carotenoids that reaches a low steady state just at the time when the incidence and prevalence of AMD begins to rise dramatically. The conclusion is further confirmed by our recent HPLC analysis of MP in 49 excised donor eyes, where we found a decline of MP levels with age (unpublished data). These results also emphasize the importance of ensuring that populations are properly age-matched when using RRS spectroscopy in case-control studies.
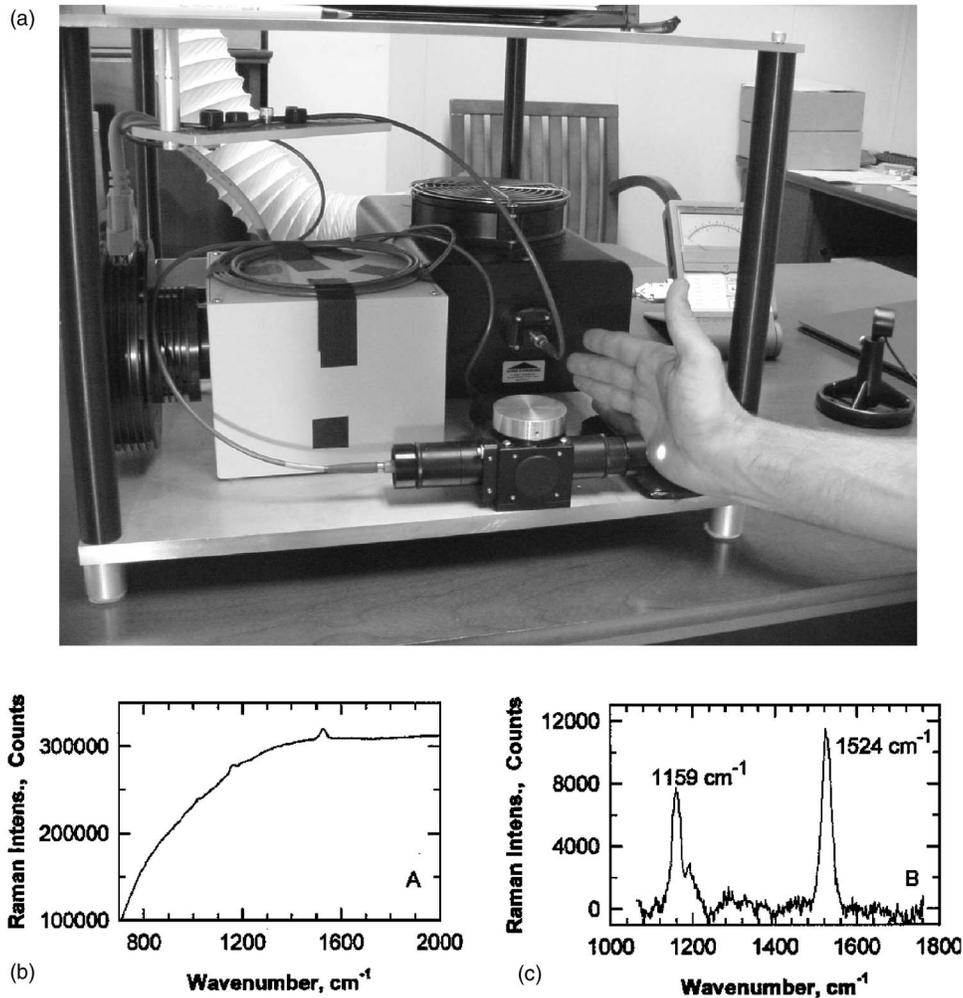
(a)

(b)

(c)

Fig. 12 (a) Skin carotenoid resonance Raman detector, showing argon laser, spectrograph, light delivery/collection module, and excitation laser spot on the palm of the hand of a subject. A typical measurement involves the placement of the palm of the hand against the window of the module and exposing the palm for about 1 min at laser intensities of ~10 mW in a 2-mm-diam spot. Carotenoid Raman signals are detected with a 2-D CCD camera integrated with the spectrograph (left side of image), and processed similar to the ocular Raman instrument. (b) Typical skin carotenoid Raman spectra measured *in vivo*. Spectrum shown on the left is spectrum obtained directly after exposure, and reveals broad, feature-less, and strong autofluorescence background of skin with superimposed sharp Raman peaks characteristic for carotenoid molecules. Spectrum at the right is difference spectrum obtained after fitting fluorescence background with a fourth-order polynomial and subtracting it from the spectrum on the left. The main characteristic carotenoid peaks are clearly resolved with good SNRs at 1159 and 1524 cm^{-1}.

An example for RRS clinical measurements of a relatively young subgroup (33 eyes), ranging in age from 21 to 29 yr is shown in Fig. 9. While age-dependent MP reductions can not yet be seen in this age group, a striking observation is the fact that the RRS-measured MP levels vary drastically between individuals (~10-fold change). Since the ocular transmission properties in this age group can be assumed to be very similar, the variations can be attributed to strongly varying MP levels. This conclusion is further supported by the fact that we see the same drastic variation between individual MP levels with flicker photometry, a technique that correlates with Raman measurements.[12,54] Subjects with extremely low carotenoid levels may be at higher risk of developing macular degeneration later in life.

We compared several different populations with significant macular pathology versus age-matched controls. AMD patients who did not regularly consume lutein or zeaxanthin supplements, had 32% lower macular carotenoid Raman measurements than age-matched controls.[6] Interestingly, AMD patients who had been consuming high-dose lutein supplements (≥ 4 mg/day) for at least 3 months after their diagnosis of AMD had macular carotenoid levels that on average would be considered normal for their age. These results are very supportive of the hypothesis that low macular carotenoid levels may be a risk factor for AMD and that macular pigment levels can be modified through supplements even in an elderly population with significant macular pathology. We also observed similar reductions in macular carotenoid levels relative to age-matched controls in smaller populations of subjects with macular dystrophies such as Stargardt disease and early onset macular drusen.[5] On the other hand, patients with retinitis pigmentosa or choroideremia, inherited dystrophies that affect the peripheral retina while sparing the fovea until very late in
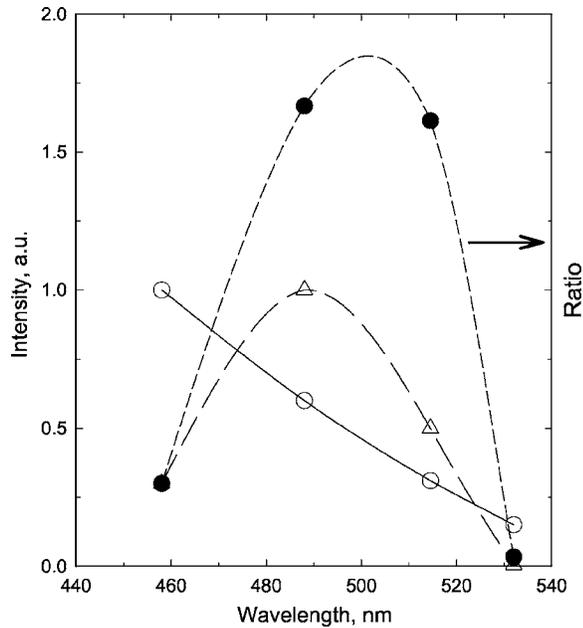
Fig. 13 Spectral dependencies of the C=C double bond RRS skin response (open triangles), skin AF background (open circles), and the resulting ratio between both responses (filled circles), measured with three blue/green argon laser excitation wavelengths and one frequency-doubled Nd:YAG laser wavelength for the inner palm stratum corneum layer of a volunteer subject. The spectral dependence of the ratio identifies an optimum excitation wavelength around 500 nm.

Fig. 14 (a) Correlation of skin resonance Raman intensity measured in the inner palm of the hand with serum carotenoids determined by HPLC, obtained for a group of 104 healthy male and female adults. Note the high correlation coefficient of $r=0.78$ ($p<0.001$). (b) Histogram of skin carotenoid resonance Raman response measured in the palm of hands for 1375 subjects, showing wide distribution of skin carotenoid levels in a large population.

the disorder, have average levels in the same range as age-matched controls.[5]

3.5 Spatial Imaging of Macular Pigments

The current version of the clinical RRS instrument measures total carotenoids in the 1-mm illuminated area centered on the fovea, but it would be very useful to also have information on the spatial distributions of the macular carotenoids. To achieve this *in vivo* spatial mapping, we developed a resonance Raman imaging system, which is shown schematically in Fig. 10(a), and described in detail elsewhere.[55] It uses parallel CCD camera arrays in conjunction with a narrow band pass, angle tunable filter. A topographic pseudocolor map of MP distribution at less than 50 μm resolution is obtained by subtracting two images: one taken with the filter aligned to transmit the 1525-cm^{-1} C=C carotenoid Raman peak, and the other with the filter slightly rotated to transmit light just a few wave numbers away. A fraction of the excitation light is split off by a BS to a second CCD camera to record an image of the excitation laser intensity distribution. Currently the procedure takes 2 s. Steady fixation of the measured eye is ensured by fixation of the fellow eye onto an alignment target provided by a red laser beam that is colinear with the Raman excitation beam. The RRS image of the macula of a volunteer is shown in Fig. 10(b), and a line plot registering the pixel intensities along a horizontal meridional is displayed in Fig. 10(c). Note the roughly circularly symmetric MP distribution in the central area of the fovea but the appearance of side bumps in peripheral areas. The integral of the Raman response over the area illuminated in this imaging technique can be correlated with the previous single-spot resonance Raman
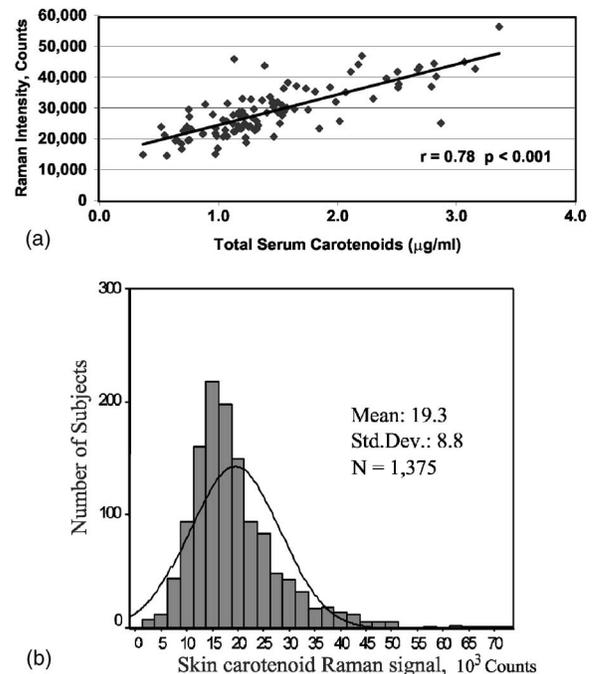
method or with extraction and HPLC analysis in case of measurements on excised eyecups. For *in vivo* imaging, the required light intensities approach the limits of safe ocular exposure at the present stage of development, however. We are hopeful that further improvements will enable us to reduce exposure levels and thus to include Raman imaging in future clinical studies of the possible role lutein and zeaxanthin in the maintenance of macular health.

4 Raman Detection of Carotenoids in Skin

4.1 Properties and Function of Skin Carotenoids

Carotenoid molecules play an important protective role in the skin's antioxidant defense system.[16] The eight most concentrated carotenoid antioxidants in human skin are lycopene, alpha-carotene, beta-carotene, β-cryptoxanthin, phytoene and phytofluene, with lycopene and the carotenes accounting for about 60–70% of total carotenoid content.[13,56] They are thought to act as scavengers for free radicals,[57] singlet oxygen,[58,59] and other harmful reactive oxygen species[60] which are all formed, e.g., by metabolic processes or by excessive exposure of skin to the UV components of sunlight. If unbalanced by a lack of antioxidants the destructive effects of reactive oxygen species and free radicals can lead to skin malignancies and disease. In animal models, carotenoids have been shown to inhibit carcinoma formation in the skin.[61] It has been shown that skin carotenoid levels are strongly and significantly correlated with carotenoid levels in plasma.[56] As is found in plasma, skin carotenoid levels are lower in smok-

ers than in nonsmokers. Carotene levels in skin are known to increase with supplementation,[62] and supplemental β-carotene is used to treat patients with erythropoietic protoporphyria, a photosensitive disorder.[63] Supplemental carotenoids have also been shown to delay erythema in normal healthy subjects exposed to UV light.[64–66] There is limited evidence that they may be protective against skin malignancies,[13] but more research is required to confirm these findings. Since carotenoids are lipophilic molecules, they are well placed in the skin to act as chain-breaking antioxidants protecting epidermal polyunsaturated fatty acids from oxygen peroxidation.[67]

Other dermal antioxidants such as superoxide dismutase, glutathione peroxidase, alpha-tocopherol, ascorbic acid, and melanins work in collaboration with carotenoids to provide skin with a defensive mechanism against free radical attack and oxidative stress.[68] Because these molecules work as a network, definitive measurement of a subset of these antioxidants provides an indication of the relative strength of the whole system. The effectiveness of this protective network can be diminished either by excessive generation of free radicals of by insufficient antioxidant molecules being supplied to the skin. The result is a state of oxidative stress where important skin constituents are exposed to free radical damage and the associated deleterious structural and chemical changes. If an individual is measured and found to have a lower than normal level of carotenoids in the skin, that person's antioxidant defense system would likely be relatively ill-equipped to balance oxidative processes compared to an individual having higher levels of antioxidants. Skin antioxidant measurements provide an opportunity for intervention strategies such as an increasing the dietary intake of fruits and vegetables, smoking cessation, and/or prescribing dietary antioxidant supplements.

For many decades, the standard technique for measuring carotenoids has been HPLC. This time-consuming and expensive chemical method works well for the measurement of carotenoids in serum, but it is difficult to perform in skin tissue since it requires biopsies of relatively large tissue volumes. Additionally, serum antioxidant measurements are more indicative of short-term dietary intakes of antioxidants rather than steady state accumulations in body tissues exposed to external oxidative stress factors such as smoking and UV light exposure. Nevertheless, the scientific basis of carotenoid function in the human body has been extensively studied for over 30 yr using the HPLC methodology.

4.2 Skin Raman Measurements

Recently, we extended resonance Raman spectroscopy to carotenoid measurements in skin and oral mucosal tissue.[14,69] This method is an appealing alternative to reflectance due to its high sensitivity and specificity, which obviates the need for complex correction models. Also, this method enables one to measure absolute carotenoid levels in these tissues, so the method does not have to rely on induced concentration changes. Although absolute levels of carotenoids are much lower in the skin relative to the macula of the human eye, laser power can be much higher, and acquisition times can be much longer to compensate. Since the bulk of the skin carotenoids are in the superficial layers of the dermis,[13] the thin-film Raman equation given earlier is still valid. Background fluorescence of the tissue can be quite high, but baseline cor-

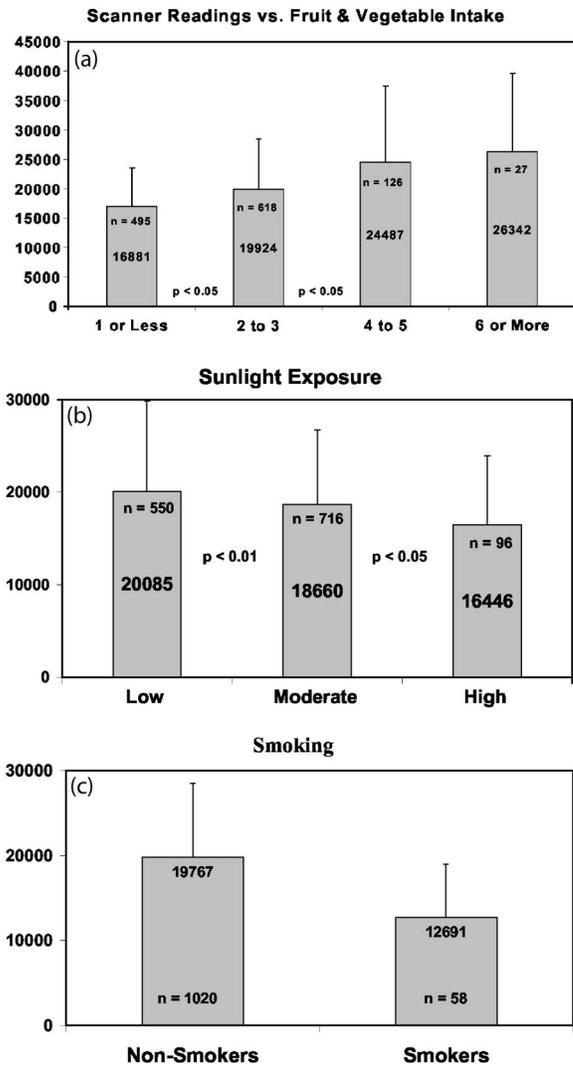**Scanner Readings vs. Fruit & Vegetable Intake**

Fig. 15 (a) Resonance Raman intensity (counts) versus reported number of daily consumed servings of fruits and vegetables, demonstrating increase of skin carotenoid concentrations with increased fruit and vegetable uptake. Means ± standard deviation (SD). (b) Resonance Raman intensity (counts) versus self-reported exposure of skin to sunlight, showing decrease of skin carotenoid levels with increased sun exposure. (c) Resonance Raman intensity (counts) in nonsmokers and cigarette smokers, showing ~30% decrease of skin carotenoid levels in smokers.

rection algorithms are still adequate to yield carotenoid resonance Raman spectra with excellent SNRs. The Raman method exhibits excellent precision and reproducibility.[13,14] Deep melanin pigmentation likely interferes with penetration of the laser beam, so measurements are best performed on the palm of the hand where pigmentation is usually quite light even in darkly pigmented individuals. Also, the stratum corneum layer in the palm of the hand is thicker ($\sim$1 to 2 mm) than the penetration depth of blue light ($\sim$several hundred micrometer), and it is bloodless.

Therefore, using this tissue site one realizes measuring conditions of a fairly homogeneous uniform layer with well-defined absorption and scattering conditions. A cross section of excised human skin, histologically stained, is shown in Fig.
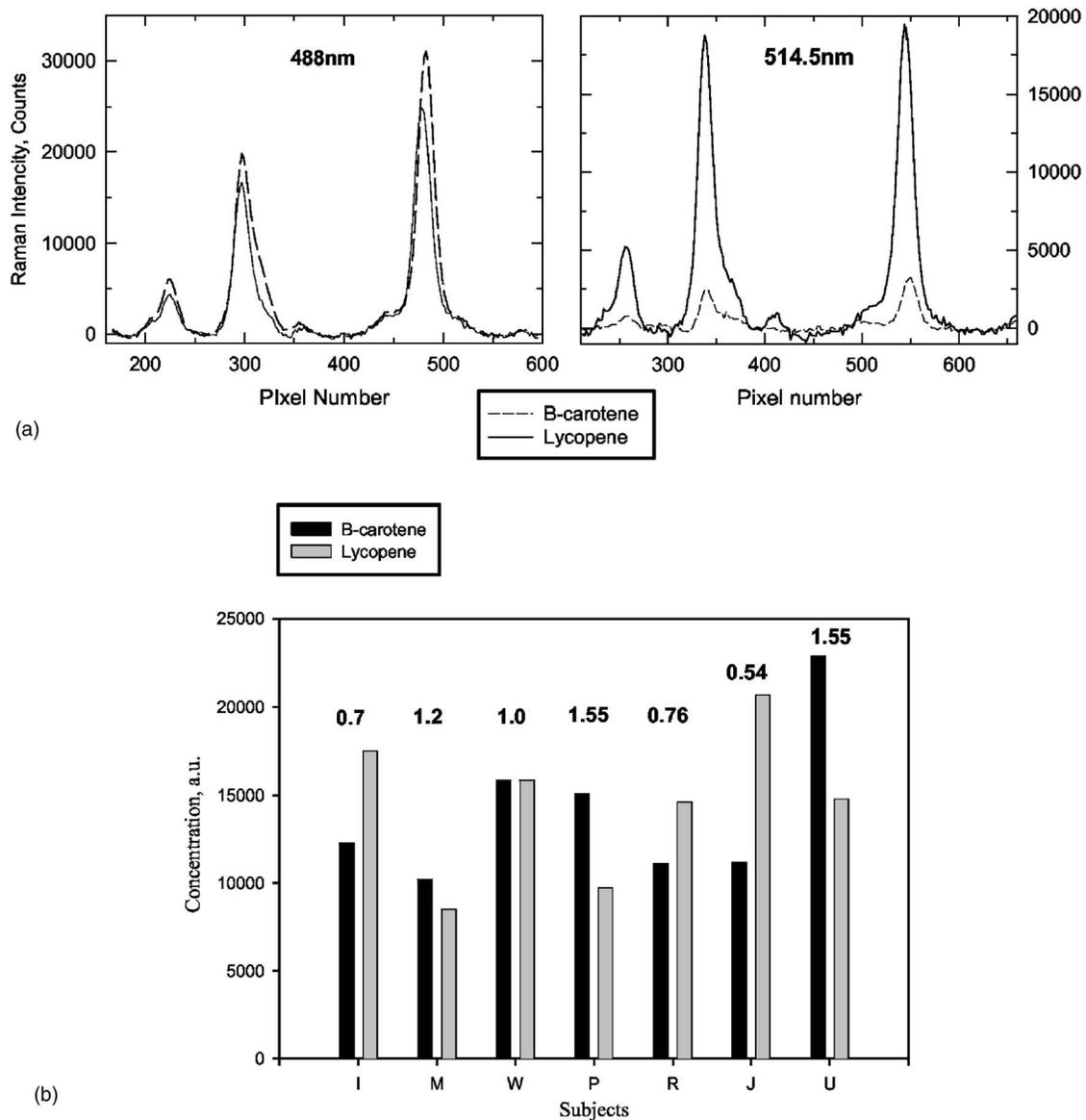
Fig. 16 (a) Resonance Raman spectrum of an acetone solution of lycopene (solid lines) and β-carotene (dotted lines), measured under argon laser excitation at 488 (left panel) and 514.5 nm (right panel). Both solutions had identical carotenoid concentrations. Raman spectra were recorded using identical excitation power and sensitivity-matched instruments. Strongest Raman peaks correspond to the stretch vibrations of the carbon single and double bonds of the molecule (at $\sim$1159 and $\sim$1525 cm^{-1}, respectively). Note strongly reduced Raman response of C=C stretch for lycopene compared to β-carotene under 514.5-nm excitation. (b) Beta-carotene and lycopene skin Raman levels measured with selective resonant Raman spectroscopy for seven subjects. Note strong intersubject variability of β-carotene to lycopene ratios (indicated above bar graphs).

11, and clearly reveals the layer structure as well as the increased homogeneity in the bloodless stratum corneum layer, where the cell nuclei are absent, and where the potentially confounding melanin concentrations are minimal as well. In fact, simple reflection spectroscopy, which is less specific and accordingly not as precise, supports these assumptions since it has already demonstrated that the stratum corneum can be used to monitor changes in carotenoid levels of the human body upon supplementation,[62] and it has also been shown that dermal carotenoid levels measured at various tissue sites are highly correlated with serum carotenoid levels.[64]

An image of the skin carotenoid Raman detection setup is shown in Fig. 12(a). The main parts of the instrument are an argon ion laser, spectrograph, and the light delivery and collection module. A typical measurement involves the placement of the palm of the hand against the window of the module and exposing the palm for about 20 s at laser intensities of $\sim$5 mW in a 2-mm-diam spot. Taking into account the 2-mm laser light spot size on the skin, this results in an intensity of 0.16 W/cm^2 at the skin surface, which is considered safe by ANSI Z136.1-2000 standards.[52] In fact, for the used laser intensity on the skin, the exposure time required for a measurement is about a factor of 1000 below the maximum allowed level of the ANSI safety standard. Carotenoid Raman signals are detected with a 2-D CCD camera integrated with

the spectrograph (left side of image). Typical skin carotenoid Raman spectra measured *in vivo* are shown in Fig. 12(b). The spectrum shown at left was obtained directly after laser exposure, and reveals a broad, featureless, and strong fluorescence background of skin with three superimposed sharp Raman peaks characteristic for the carotenoid molecules at 1015, 1159, and 1524 cm^{-1}. The spectrum shown at right represents the Raman spectrum obtained after fitting the fluorescence background with a fifth-order polynomial and subtracting if from the unprocessed spectrum, thus revealing the frequency region of the two strongest carotenoid peaks, at 1159 and 1524 cm^{-1} at an expanded scale. Strong carotenoid Raman responses were obtained also for oral mucosal tissue.[14]

To determine the excitation conditions for the best possible ratio between skin carotenoid Raman signal and AF background signal, we tested several blue-green argon laser wavelengths and the 530-nm wavelength of a frequency-doubled Nd:YAG laser as excitation sources. The result of these measurements is shown in Fig. 13. With increasing excitation wavelength, the AF background decreases monotonically while the Raman response reaches a maximum at the ~490-nm excitation wavelength. The convoluted response is seen to be optimum for an excitation wavelength of ~500 nm, which fortunately is close in wavelength to readily available laser sources at 488 nm.

We found that as with reflectometry results reported in the literature,[64] relatively high levels of skin carotenoids are measured by the Raman method on the forehead and on the palm of the hand, while other body areas are significantly lower.[13,70] To check the validity of the skin Raman measurements, we carried out a study involving a group of 104 healthy male and female human volunteers, where we compared HPLC-derived carotenoid levels of fasting serum with Raman skin levels measured in the inner palm. We obtained[71] a highly significant correlation ($p < 0.001$) with a correlation coefficient of 0.78. The main result of this study is shown in Fig. 14(a). Measurements of large populations with the Raman device have demonstrated a widely varying concentrations of carotenoid levels in the palm of the hand.[16] Field studies were recently carried out where a population of 1375 healthy subjects could be screened within a period of several weeks.[71] The results are shown in Fig. 14(b), demonstrating a bell-shaped distribution of skin carotenoid concentrations with a large variation throughout the population. Analysis of the data confirmed a pronounced positive relationship between self-reported fruit and vegetable intake (a source of carotenoids) and skin Raman response [Fig. 15(a)]. Furthermore, the study showed that people with habitual high sunlight exposure have significantly lower skin carotenoid levels than people with little sunlight exposure, independent of their carotenoid intake or dietary habits [Fig. 15(b)], and that smokers had dramatically lower levels of skin carotenoids as compared to nonsmokers [Fig. 15(c)]. When analyzed by a chemical assay based on urinary malondialdehyde excretion, an indicator of oxidative lipid damage, people with high oxidative stress had significantly lower skin carotenoid levels than people with low oxidative stress. Again, this relationship was not confounded by dietary carotenoid intakes, which were similar in both groups. These observations provide evidence that skin carotenoid resonance Raman readings might be useful as a surrogate
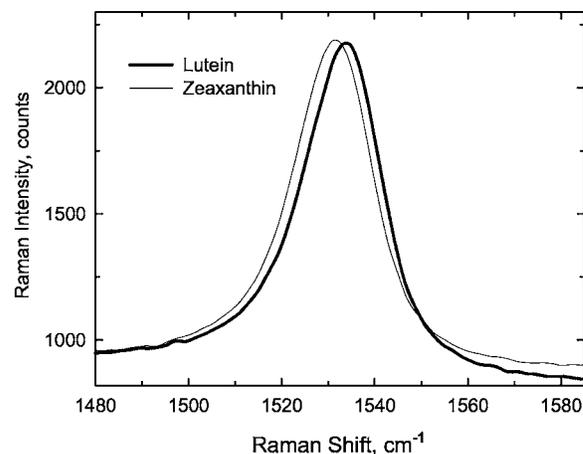

Fig. 17 C=C double-bond Raman spectra of lutein (thick line) and zeaxanthin (thin line) dissolved in methanol and measured at room temperature under excitation with 488-nm light. A small (~2.5 cm^{-1}) but readily detectable chemical shift of the double-bond stretching frequency in these two very similar compounds, which differ in effective conjugation length by one double bond, could be potentially used for selective detection of each carotenoid in retinal tissue.

marker for general antioxidant status,[16] which was recently suggested for plasma carotenoids as well.[72] The recent availability of a commercial, portable resonance Raman instrument for skin carotenoids (BioPhotonic Scanner™, Pharmanex LLC, Provo, Utah) facilitates further nutrition studies.

Studies are also underway to determine whether low skin Raman measurements may be associated with increased risk of various cancers.[17] Initial studies have demonstrated that lesional and perilesional Raman carotenoid intensities of cancerous and precancerous skin lesions are significantly lower than in region-matched skin of healthy subjects.[13]

4.3 Selective Detection of Carotenes and Lycopene in Human Skin

In all previous Raman measurements of dermal carotenoids we measured the composite level of the long-chain carotenoid species since they are all simultaneously excited under the used conditions, and all contribute to the overall Raman response. The increased conjugation length in lycopene compared to the other carotenoids in skin produces a small (~10 nm) but distinguishable red shift of the absorption band that can be used to measure lycopene independently of the other carotenoids.[15] There is considerable interest in a specific role for lycopene in prevention of prostate cancer and other diseases,[66,73] and a noninvasive biomarker for lycopene consumption would be of tremendous utility. As seen in Fig. 16(a) for solutions of lycopene and β-carotene, the resonance Raman response has approximately the same strengths under 488-nm excitation. However, under excitation with 514.5 nm, the response is about 6 times higher for lycopene. Therefore, it is possible to measure the individual responses in a mixture of both by measuring in addition to the 488- and 514.5-nm responses, and taking into account the relative carotenoid contributions in the resulting spectra.[15] In initial experiments with seven volunteer subjects, we measured the skin Raman response from the stratum corneum of the palm
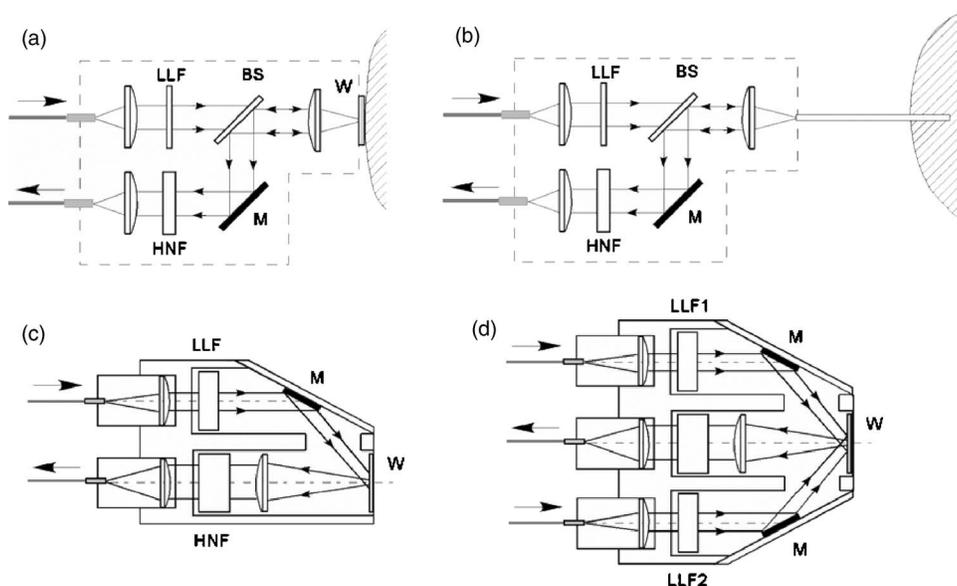
Fig. 18 Handheld optical probes used for RRS carotenoid detection of human and other biological tissues: LLF, laser line filter; HNF, holographic notch filter; M, mirror; W, optical window; BS, beamsplitter. (a) and (b) Probes use colinear excitation-detection geometry and can be used to sample near the tissue surface or inside the tissue if interfaced with a 1-mm-diam fiber needle. (c) and (d) Raman probes use oblique excitation-detection geometry, having the advantage of lowering confounding tissue fluorescence and eliminating the need for a dichroic beam splitter otherwise placed inside the probe. (d) Two-excitation channel probe is used for selective detection of lycopene and carotenes, respectively, in human skin and ensures identical probe volume for each wavelength during measurements.

of the hand using such a dual-wavelength carotenoid Raman detection instrument and demonstrated large variations in individual skin lycopene levels. The most important result of this experiment is summarized in Fig. 16(b), where the individual lycopene and carotene levels are indicated together with the lycopene/carotene ratio for each subject. Obviously, there is a strong, almost threefold variation in the carotene-to-lycopene ratio in the measured subjects, ranging from 0.54 to 1.55. This means that substantially different carotenoid compositions exist in human skin, with some subjects exhibiting almost twice the concentration of lycopene compared to carotene, and other subjects showing the opposite effect. This behavior could reflect different dietary patterns regarding the intake of lycopene or lycopene-containing vegetables, or it could point toward differing abilities between subjects to accumulate these carotenoids in the skin.

Besides taking advantage of the differences in RRS excitation profiles for different carotenoid species, an alternative approach for selective and quantitative detection of individual carotenoids in a mixed sample may be based on RRS detection of changes in the vibrational carbon stretch frequencies. These "chemical shifts," caused by the slightly differing masses and force constants of the molecules, are usually very small due to the high similarity of the molecular structures. An exception is the case of phytofluene in which the $C\!\!=\!\!C$ double frequency is shifted to higher frequencies by almost 80 cm^{-1} as compared to β-carotene (see Fig. 2). Motivated by the desire to selectively detect the important macular pigments lutein and zeaxanthin, we measured the chemical shift of these two compounds in solution as a first test. Any attempt to selectively detect these carotenoids using differences in absorption behavior would be practically impossible due to the extremely close similarity in their absorption transitions (see

Fig. 1). The result is shown in Fig. 17 and reveals a shift of $\sim$2.5 cm^{-1}, detectable with a medium-resolution (1/2 m) grating spectrograph even at room temperature of the sample. This makes it potentially possible to separately detect these important molecules in human retinal tissue.

4.4 Optical Probes for RRS

Depending on the tissue of interest for carotenoid detection and the desire to selectively measure individual carotenoids, we are developing optical probe designs differing in the stray light rejection properties and number of excitation and/or detection channels. Four major probe designs are shown in Fig. 18, already published to some extent elsewhere.[74] Probes shown in Figs. 18(a) and 18(b) use colinear excitation-detection geometry and can be used to sample near the tissue surface or inside the tissue if interfaced with an appropriate optical fiber "needle." As needles we tested $\sim$1-mm-diam fibers and were able to detect carotenoid RRS responses in fiber lengths up to about 30 cm, at which RRS scattering from fiber compounds started to interfere with carotenoid detection. Raman probes shown in Figs. 18(c) and 18(d) use oblique excitation-detection geometries, having the advantage of lowering confounding tissue fluorescence and eliminating the need for a dichroic beam splitter otherwise placed inside the probe. The two-excitation channels of probe in Fig. 18(d) are used for selective detection of lycopene and carotenes, respectively, in human skin and ensure identical probe volume for each wavelength during the measurements.

5 Conclusions

RRS spectroscopy appears well suitable for quantitative detection of carotenoid antioxidants in living human tissue. It is

highly specific, sensitive, and precise and it enables one to rapidly assess dermal carotenoid content in large populations with excellent correlation to serum levels. Regarding MP measurements, it can quickly and objectively assess composite lutein and zeaxanthin scores in averaged integral measurements and it also has good potential to map and quantify the complete MP distribution. To our knowledge there are no serious confounding factors for the technology in our applications. Since RRS takes absolute measurements of carotenoid responses, care must be taken, of course, to eliminate or at least minimize interfering media opacities. This is particularly important when the interest lies in comparing carotenoid tissue levels between different subjects having potentially differing media opacities. In ocular Raman measurements, problems could occur, in principle, from yellowing of the lens on cataract formation, leading to interfering absorption. However, since the Raman measurements are carried out in a wavelength range that is located on the long-wavelength shoulder of cataract-induced absorption changes, these influences are relatively weak.[75] As a precaution, we avoid media-opacity-related problems by limiting the measurements to subjects with visual acuity better than 20/80. A correlation of our MP Raman responses with data derived by HPLC and flicker techniques is proof that these precautions are adequate. In dermal Raman measurements, potentially confounding factors are melanin and hemoglobin absorptions. In our dermal application, we avoid potential interferences by measuring the stratum corneum layer of the palm. At this site, the tissue is thicker than the penetration depth of the laser, thus avoiding absorption of hemoglobin. Furthermore, the stratum corneum tissue is free of melanin. A correlation of our Raman-derived carotenoid data with HPLC-derived serum levels again confirms the validity of the carotenoid Raman detection technique in the physiologically relevant concentration range under these measuring conditions (see Figs. 8 and 14). Any tissue opacities are of course less problematic in longitudinal studies involving the same subjects, for example, in studies designed to investigate changes of MP or dermal carotenoid levels on dietary changes or influences of external stress. We believe that carotenoid RRS detection has exciting application potential. In the nutritional supplement industry, it is already being used as an objective, portable device for the monitoring of effect of carotenoid-containing supplements on skin tissue carotenoid levels. In ophthalmology, it may become a fast screening method for MP levels in the general population; and in cancer epidemiology, it may serve as a noninvasive novel biomarker for fruit and vegetable intake, replacing costly plasma carotenoid measurements with inexpensive and rapid skin Raman measurements. Last, due to its capability to selectively detect lycopene, the technology may be useful to investigate a specific role of lycopene in the prevention of prostate cancer and other diseases.

Acknowledgments

References

1. Y. Koyama, "Resonance Raman spectroscopy," in *Carotenoids*, Vol. **1B**, *Spectroscopy*, G. Britton, Liaaen-Jensen, and H. Pfander, Eds., pp. 135–146, Birkhäuser, Basel (1995).
2. P. S. Bernstein, M. D. Yoshida, N. B. Katz, R. W. McClane, and W. Gellermann, "Raman detection of macular carotenoid pigments in intact human retina," *Invest. Ophthalmol. Visual Sci.* **39**, 2003–2011 (1998).
3. W. Gellermann, I. V. Ermakov, M. R. Ermakova, R. W. McClane, D. Y. Zhao, and P. S. Bernstein, "*In vivo* resonant Raman measurement of macular carotenoid pigments in the young and the aging human retina," *J. Opt. Soc. Am. A* **19**, 1172–1186 (2002).
4. I. V. Ermakov, M. R. Ermakova, P. S. Bernstein, and W. Gellermann, "Macular pigment Raman detector for clinical applications," *J. Biomed. Opt.* **9**(1), 139–148 (2004).
5. D.-Y. Zhao, S. W. Wintch, I. V. Ermakov, W. Gellermann, and P. S. Bernstein, "Resonance Raman measurement of macular carotenoids in retinal, choroidal, and macular dystrophies," *Arch. Ophthalmol. (Chicago)* **121**, 967–972 (2003).
6. P. S. Bernstein, D. Y. Zhao, S. W. Wintch, I. V. Ermakov, and W. Gellermann, "Resonance Raman measurement of macular carotenoids in normal subjects and in age-related macular degeneration patients," *Monist* **109**, 1780–1787 (2002).
7. R. E. Hogg, E. E. Johnston, R. S. Anderson, M. R. Stevenson, and U. Chakravarthy, "Macular pigment concentration and retinal morphology," in *Proc. ARVO Conf. 2005*, Fort Lauderdale, FL, Abstract # 1778/B547, available at http://www.arvo.org (2005).
8. G. Monterosso, M. Sartore, S. Vujosevic, E. Pilotto, F. Cavarzeran, and S. Piermarocchi, "Resonance Raman measurement of macular carotenoids in a European population," in *Proc. ARVO Conf. 2005*, Fort Lauderdale, FL, Abstract # 1758/B527, available at http://www.arvo.org (2005).
9. O. M. O'Donovan, J. Nolan, K. Neelam, and S. Beatty, "Measurement of macular pigment: Raman spectroscopy versus heterochromatic flicker photometry," in *Proc. ARVO Conf. 2005*, Ft. Lauderdale, FL, Abstract # 1783/B552, available at http://arvo.org (2005).
10. A. Obana, Y. Gohto, T. Hiramitsu, T. Hirano, Y. Hotta, T. Nakagami, H. Qui, K. Iseki, S. Mizuno, and P. S. Bernstein, "Resonance Raman spectroscopic measurement of macular carotenoids in Japanese population," in *Proc. ARVO Conf. 2005*, Ft. Lauderdale, FL, Abstract # 1572/B341, available at http://arvo.org (2005).
11. K. Neelam, J. Nolan, O. O'Donovan, K. Au Eong, and S. Beatty, "Macular pigment levels following successful macular hole surgery," in *Proc. ARVO Conf. 2005*, Ft. Lauderdale, FL, Abstract # 1777/B546, available at http://arvo.org (2005).
12. K. Neelam, N. O'Gorman, J. Nolan, O. O'Donovan, H. B. Wong, K. G. Au Eong, and S. Beatty, "Measurement of macular pigment: Raman spectroscopy versus heterochromatic flicker photometry," *Invest. Ophthalmol. Visual Sci.* **46**, 1023–1032 (2005).
13. T. R. Hata, T. A. Scholz, I. V. Ermakov, R. W. McClane, F. Khachik, W. Gellermann, and L. K. Pershing, "Non-invasive Raman spectroscopic detection of carotenoids in human skin," *J. Invest. Dermatol.* **115**, 441–448 (2000).
14. I. V. Ermakov, M. R. Ermakova, R. W. McClane, and W. Gellermann, "Resonance Raman detection of carotenoid antioxidants in living human skin," *Opt. Lett.* **26**, 1179–1181 (2001).
15. I. V. Ermakov, M. R. Ermakova, W. Gellermann, and J. Lademann, "Non-invasive selective detection of lycopene and beta-carotene in human skin using Raman spectroscopy," *J. Biomed. Opt.* **9**, 332–338 (2004).
16. W. Gellermann, I. V. Ermakov, R. W. McClane, T. A. Scholz, P. S. Bernstein, "Noninvasive laser Raman detection of carotenoid antioxidants in skin," *Cosmet. Dermatol.* **15**(9), 65–68 (2002).
17. J. Lademann, personal communication; see also http://cancer.med.upenn.edu/resources/article.cfm?c=3&s=8&ss=23&id=9647&month=05&year=2003.
18. A. P. Shreve, J. K. Trautman, T. G. Owens, and A. C. Albrecht, "Determination of the S2 lifetime of β-carotene," *Chem. Phys. Lett.* **178**, 89–96 (1991).
19. R. A. Bone, J. T. Landrum, and S. L. Tarsis, "Preliminary identification of the human macular pigment," *Vision Res.* **25**, 1531–1535 (1985).
20. G. J. Handelman, D. M. Snodderly, A. J. Adler, M. D. Russett, and E. A. Dratz, "Measurement of carotenoids in human and monkey retinas," *Methods Enzymol.* **213**, 220–230 (1992).

21. W. Schalch, P. Dayhaw-Barker, and F. M. Barker, "The carotenoids of the human retina," in *Nutritional and Environmental Influences on the Eye*, A. Taylor, Ed., pp. 215–250, CRC Press, Boca Raton, FL (1999).

22. D. M. Snodderly, "Evidence for protection against age-related macular degeneration by carotenoids and antioxidant vitamins," *Am. J. Clin. Nutr. Suppl.* **62**, 1448S–1461S (1995).

23. Eye Disease Case Control Study Group, "Antioxidant status and neovascular age-related macular degeneration," *Arch. Ophthalmol. (Chicago)* **111**, 104–109 (1993).

24. J. M. Seddon, U. A. Ajani, R. D. Sperduto, R. Hiller, N. Blair, T. C. Burton, M. D. Farber, E. S. Gragoudas, J. Haller, D. T. Miller, L. A. Yannuzzi, and W. Willet, "Dietary carotenoids, vitamins A, C, and E, and advanced age-related macular degeneration," *J. Am. Med. Assoc.* **272**, 1413–1420 (1994).

25. R. A. Bone, J. T. Landrum, S. T. Mayne, C. M. Gomez, S. E. Tibor, and E. E. Twaroska, "Macular pigment density in donor eyes with and without AMD: a case-control study," *Invest. Ophthalmol. Visual Sci.* **42**, 235–240 (2001).

26. S. Beatty, I. J. Murray, D. B. Henson, D. Carden, H.-H. Koh, and M. E. Boulton, "Macular pigment and risk for age-related macular degeneration in subjects from a northern European population," *Invest. Ophthalmol. Visual Sci.* **42**, 439–446 (2001).

27. D. M. Snodderly, J. D. Auran, and F. C. Delori, "The macular pigment, I: absorbance spectra, localization, and discrimination from other yellow pigments in primate retinas," *Invest. Ophthalmol. Visual Sci.* **25**, 660–673 (1984).

28. P. S. Bernstein and N. B. Katz, "The role of ocular free radicals in age-related macular degeneration," in *Environmental Stressors: Effects on Lung, Skin, Eye and Immune System Function*, J. Fuchs and L. Packer Eds., pp. 423–456, Marcel Dekker, New York (2000).

29. S. Beatty, H.-H. Koh, D. Henson, and M. Boulton, "The role of oxidative stress in the pathogenesis of age-related macular degeneration," *Surv. Ophthalmol.* **45**, 115–134 (2000).

30. V. M. Reading and R. A. Weale, "Macular pigment and chromatic aberration," *J. Am. Optom. Assoc.* **64**, 231–234 (1974).

31. B. R. Hammond, Jr., B. R. Wooten, and D. M. Snodderly, "Individual variations in the spatial profile of human macular pigment," *J. Opt. Soc. Am. A* **14**, 1187–1196 (1997).

32. D. M. Snodderly and B. R. Hammond, "*In vivo* psychophysical assessment of nutritional and environmental influences on human ocular tissues: lens and macular pigment," in *Nutritional and Environmental Influences on the Eye*, A. Taylor, Ed., pp. 251–273, CRC Press, Boca Raton, FL (1999).

33. J. S. Werner, M. L. Bieber, and B. E. Schefrin, "Senescence of foveal and parafoveal cone sensitivities and their relations to macular pigment density," *J. Opt. Soc. Am. A* **17**, 1918–1932 (2000).

34. B. R. Hammond and M. Caruso-Avery, "Macular pigment optical density in a southwestern sample," *Invest. Ophthalmol. Visual Sci.* **41**, 1492–1497 (2000).

35. D. van Norren and L. F. Tiemeijer, "Spectral reflectance of the human eye," *Vision Res.* **26**, 313–320 (1986).

36. F. C. Delori and K. P. Pflibsen, "Spectral reflectance of the human ocular fundus," *Appl. Opt.* **28**, 1061–1077 (1989).

37. J. van de Kraats, T. T. J. M. Berendshot, and D. van Norren, "The pathways of light measured in fundus reflectometry," *Vision Res.* **36**, 2229–2247 (1996).

38. T. Berendshot, J. van de Kraats, and D. van Norren, "Three methods to measure macular pigment compared in a lutein intake study," *Invest. Ophthalmol. Visual Sci.* **39**, S314 (1999) [Association for research in Vision and Ophthalmology (ARVO) Abstract No. 1665].

39. P. E. Kilbride, K. R. Alexander, M. Fishman, and G. A. Fishman, "Human macular pigment assessed by imaging fundus reflectometry," *Vision Res.* **29**(6), 663–674 (1989).

40. R. H. Webb, G. W. Hughes, and O. Pomerantzeff, "Flying spot TV ophthalmoscope," *Appl. Opt.* **19**, 2991–2997 (1980).

41. R. H. Webb, G. W. Hughes, and F. C. Delori, "Confocal scanning laser ophthalmoscope," *Appl. Opt.* **26**, 1492–1499 (1987).

42. D. van Norren and J. van de Kraats, "Imaging retinal densitometry with a confocal scanning ophthalmoscope," *Vision Res.* **29**, 1825–1830 (1989).

43. A. E. Elsner, S. A. Burns, F. C. Delori, and R. H. Webb, "Quantitative reflectometry with the SLO," in *Laser Scanning Ophthalmoscopy and Tomography*, J. E. Nasemann and R. O. W. Burk, Eds., pp. 109–121, Quintessenz-Verlag, Berlin (1990).

44. A. E. Elsner, S. A. Burns, G. W. Hughes, and R. H. Webb, "Reflectometry with a scanning laser ophthalmoscope," *Appl. Opt.* **31**, 3697–3710 (1992).

45. A. E. Elsner, S. A. Burns, E. Beausencourt, and J. J. Weiter, "Foveal cone photopigment distribution: small alterations associated with macular pigment distribution," *Invest. Ophthalmol. Visual Sci.* **39**, 2394–2404 (1998).

46. D. Schweitzer, M. Hammer, and M. Scibor, "Imaging spectrometry in ophthalmology—principle and applications in microcirculation and in investigation of pigments," *Invest. Ophthalmol. Visual Sci.* **39**, 2001–2011 (1998).

47. F. C. Delori, "Macular pigment density measured by reflectometry and fluorophotometry," in *Ophthalmic and Visual Optics and Noninvasive Assessment of the Visual System*, OSA Technical Digest Series, Vol. **3**, pp. 240–243, Optical Society of America, Washington, DC (1993).

48. F. C. Delori, D. G. Goger, B. R. Hammond, D. M. Snodderly, and S. A. Burns, "Macular pigment density measured by autofluorescence spectrometry: comparison with reflectometry and heterochromatic flicker photometry," *J. Opt. Soc. Am. A* **18**, 1212–1230 (2001).

49. T. T. J. M. Berendshot, R. A. Goldbohm, W. A. A. Kloepping, J. van de Kraats, J. Van Norel, and D. van Norren, "Influence of lutein supplementation on macular pigment, assessed with two objective techniques," *Invest. Ophthalmol. Visual Sci.* **41**, 3322–3326 (2000).

50. I. V. Ermakov, R. W. McClane, W. Gellermann, and P. S. Bernstein, "Resonance Raman detection of macular pigment levels in the living human retina," *Opt. Lett.* **26**, 202–204 (2001).

51. P. S. Bernstein, W. Gellermann, and R. W. McClane, "Method and system for measurement of macular carotenoid levels," U.S. Patent No. 5,873,831 (1999).

52. American National Standards Institute, "American national standard for safe use of lasers," ANSI Z136.1-2000, Sec. 8.3, Laser Institute of America, Orlando, FL (2000).

53. S. Beatty, I. J. Murray, D. B. Henson, D. Carden, H. Koh, and M. E. Boulton, "Macular pigment and risk for age-related macular degeneration in subjects from a Northern European population," *Invest. Ophthalmol. Visual Sci.* **42**, 439–446 (2001).

54. P. S. Bernstein, D.-Y. Zhao, M. Sharifzadeh, I. V. Ermakov, and W. Gellermann, "Resonance Raman measurement of macular carotenoids in the living human eye," *Arch. Biochem. Biophys.* **430**, 163–169 (2004).

55. W. Gellermann, I. V. Ermakov, R. W. McClane, and P. S. Bernstein, "Raman imaging of human macular pigments," *Opt. Lett.* **27**, 833–835 (2002).

56. F. Böhm, J. H. Tinkler, and T. G. Truscott, "Carotenoids protect against cell membrane damage by the nitrogen dioxide radical," *Clin. Cancer Res.* **1**, 98–99 (1995).

57. C. S. Foote and R. W. Denny, "Chemistry of singlet oxygen, VIII. Quenching by β-carotene," *J. Am. Chem. Soc.* **90**, 6233–6235 (1968).

58. A. Farmillo and F. Wilkinson, "On the mechanism of quenching of singlet oxygen in solution," *Photochem. Photobiol.* **18**, 447–450 (1973).

59. P. F. Conn, W. Schalch, and T. G. Truscott, "The singlet oxygen and carotenoid interaction," *J. Photochem. Photobiol., B* **11**, 41–47 (1991).

60. L. C. Chen, L. Sly, C. S. Jones, R. De Tarone, L. M. Luca, "Differential effects of dietary β-carotene on papilloma and carcinoma formation induced by an initiation-promotion protocol in SENCAR mouse skin," *Carcinogenesis* **14**, 713–717 (1993).

61. Y. M. Peng, Y. S. Peng, Y. Lin, T. Moon, D. J. Roe, and C. Ritenbaugh, "Concentrations and plasma-tissue-diet relationships of carotenoids, retinoids, and tocopherols in humans," *Nutr. Cancer* **23**, 233–246 (1995).

62. M. R. Prince and J. K. Frisoli, "Beta-carotene accumulation in serum and skin," *Am. J. Clin. Nutr.* **57**, 175–181 (1993).

63. M. M. Mathews-Roth, "Carotenoids in erythropoietic protoporphyria and other photosensitivity diseases," *Ann. N.Y. Acad. Sci.* **691**, 127–138 (1993).

64. W. Stahl, U. Heinrich, H. Jungmann, H. Sies, and H. Tronnier, "Carotenoids and carotenoids plus vitamin E protect against ultraviolet light-induced erythema in humans," *Am. J. Clin. Nutr.* **71**, 795–798 (2000).

65. J. Lee, S. Jiang, N. Levine, and R. Watson, "Carotenoid supplementation reduces erythema in human skin after simulated solar radiation exposure," *Proc. Soc. Exp. Biol. Med.* **223**, 170–174 (2000).

66. E. Giovannucci, "Tomatoes, tomato-based products, lycopene, and cancer: review of the epidemiological literature," *J. Natl. Cancer Inst.* **91**, 317–331 (1999).

67. H. I. Krinsky and S. M. Deneke, "The interaction of oxygen and oxyradicals with carotenoids," *JNCI, J. Natl. Cancer Inst.* **69**, 205–210 (1982).

68. D. P. T. Steenvorden and G. M. J. Beijerbergen van Henegouwen, "The use of endogenous antioxidants to improve photoprotection," *J. Photochem. Photobiol., B* **41**, 1–10 (1997).

69. W. Gellermann, P. S. Bernstein, and R. W. McClane, "Method and apparatus for noninvasive measurement of carotenoids and related chemical substances in biological tissue," U.S. Patent No. 6,205,354 B1 (2001).

70. S. Alaluf, U. Heinrich, H. Tronnier, and S. Wiseman, "Dietary carotenoids contribute to normal human skin color and photosensitivity," *J. Nutr.* **26**, 1179–1181 (2002).

71. W. Gellermann, J. A. Zidichouski, C. R. Smidt, and P. S. Bernstein, "Raman detection of carotenoids in human tissue, in *Carotenoids and Retinoids: Molecular Aspects and Health Issues*, L. Packer, K. Krämer, U. Obermüller-Jervic, and H. Sies, Eds., Chapter 6, pp. 86–114, AOCS Press, Champaign, Illinois (2005).

72. A. Svilaas, A. K. Sakhi, L. F. Andersen, T. Svilaas, E. C. Ström, D. R. Jacobs, Jr., L. Ose, and R. Blomhoff, "Intakes of antioxidants in coffee, wine, and vegetables are correlated with plasma carotenoids in humans," *J. Nutr.* **134**, 562–567 (2004).

73. A. V. Rao, "Lycopene, tomatoes, and the prevention of coronary heart disease," *Exp. Biol. Med.* **227**(10), 908–913 (2002).

74. A. Mahadevan-Jansen, R. Richards-Kortum, and M. F. Mitchell, "Spectroscopic probe for in vivo measurement of Raman signals," U.S. Patent No. 5,842,995 (Dec. 1, 1998).

75. N. P. A. Zagers and D. van Norren, "Absorption of the eye lens and the macular pigment derived from the reflectance of cone photoreceptors," *J. Opt. Soc. Am. A* **21**, 2257–2268 (2004).